Analysis of Micro Machinable Piezoelectrically Driven One Dimensional Flexural Transducers

A. Rønnekleiv*, P. E. Roche, and B. T. Khuri-Yakub

E. L. Ginzton Laboratory, Stanford University, CA 94305, USA

**On leave during 1996/97 from Div. of Physical Electronics, NTNU, Trondheim, Norway*

Abstract **Flexural piezoelectrically driven transducers are of interest as they may couple efficiently to fluids, and could be realized for high frequencies using michromachining techniques. Arrays of essentially one dimensional elements are attractive as they may have small inactive boundary areas. We present an analytical theory for such elements. It may handle arbitrarily layered plate structures with one or more piezoelectric layers included, varying along the plate, and is valid also for higher harmonics. It includes shear deformation, effects of residual stress in the plate, and bending effects at height differences between plate elements.**

The analysis is compared both to experiments on a low frequency (140 kHz) PZT brass structure, and to FEM analysis. FEM is also used to determine realistic edge boundary conditions for the structure. The theory matches well with the FEM analysis for plate resonance's, and is in reasonable agreement with experiments.

Introduction

The use of thin flexing plates, or membranes, which are piezoelectrically driven, to make ultrasonic flexural transducers is well known [1-2]. The silicon micromachining technology combined with methods of making high quality piezoelectric thin films [4] should make it possible to realize such transducers at high frequencies and with high complexity. This could possibly lead to high frequency ultrasonic array transducers which are steerable in 1, 1.5, or even 2 dimensions for different purposes including medical imaging. Such structures are normally analyzed using FEM analysis to achieve high accuracy.

Here we present an analytical model for a one dimensional structure which takes into account a number of effects which are often ignored. This makes the model match well with FEM analysis. FEM analysis is however needed to model the action of the supports of the membranes, and such analysis is given for a test structure. The model could be extended to two dimensional plates. However the one dimensional model is a good approximation for elongated rectangular plates, which are ideal building blocks for 1 and 1.5 dimensional arrays.

The analytical model is compared to FEM analysis and to experiments on a test structure built from brass and PZT by conventional bonding and grinding techniques.

Theory

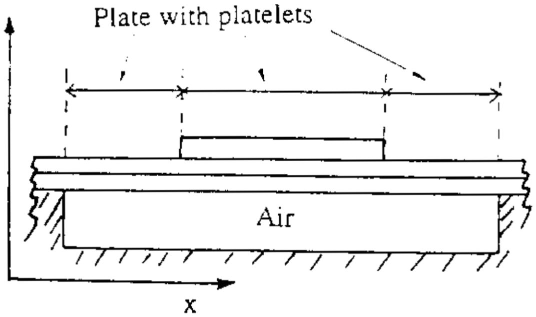

Figure 1: Cross section of an element

The modeled flexural transducer consists of a set of stripe like composite plates which are uniform in y direction, see Fig. 1. They are supported on both sides in y-direction and may consist of several platelets in x-direction, each of which is a sandwich in z-direction of different piezoelectric or non piezoelectric films. The analytical model includes the effect of bending, shear deformation, and both constant and time varying longitudinal strain in the plate. The longitudinal strain in the plate is not treated as a wave, but rather in an quasistatic approximation where acceleration forces are neglected, as the longitudinal waves will normally have wave velocities that are much higher than the flexural waves accounting for of the membrane deflection. The force given by the longitudinal strain is of importance as it will couple to bending of the plate if any of the platelets are supported asymmetrically with respect to their neutral axis. This is often the case at the edges, or between the platelets due to height differences. Piezoelectric films in the platelet will in most cases couple both to bending and to longitudinal strain of the platelet.

Further the effect of cos-shaped pressure waves in an adjoin-ing fluid is included to allow calculation of radiation into a fluid. Radiation into a fluid is not further detailed in the paper.

The piezoelectric is assumed to have essentially the

0-7803-4153-8/97/$10.00

symmetry of PZT, with the polar axis normal to the platelet. It may either be without metalization, or metalized on one or both sides, in the latter case with a voltage difference which is the applied voltage V of the transducer. We will describe the piezoelectric by its elastic moduli for normal strain in x direction at constant D field, C_p^D, and at constant electric field, C_p^E, an effective piezoelectric coupling coefficient e_{eff} (at constant E field), connecting strain in x direction and D field in z direction, and the dielectric constant in z direction at constant strain in x and y directions, ε_{eff}.

In bending or longitudinal stretching of the platelet it is assumed that the deformation in y direction and the stress in z direction is zero, as is normal in plate theory. Hence the bending stiffness D_b is obtained as is normal in plate theory, but with special attention to the piezoelectric. Regions of the piezoelectric which are not metalized, or only metalized on one side, will have the piezoelectric stiffening of the material, and hence c_p is always used. For metalized regions of the piezoelectric the situation is more complex. We assume that the strain will vary linearly with z. For metalized regions of the piezoelectric at a constant voltage, we decompose the strain in a term constant in z, equal to the average strain, and the remainder which will vary linearly with z and be zero at the center of the film. For the first strain the piezoelectric will have a stiffness C_p^E, as if it is shorted. Hence C_p^E should be used for the contribution to D_b given by the moment due to the uniform stretching of the piezoelectric. For the second strain part, the antisymmetric component, the metalization will not be able to short out the E-fields, which are also antisymmetric, and hence the effective stiffness for bending of the film about its center line is C_p^D.

Fringing fields in the piezoelectric outside the metalized regions are not treated rigorously, but their effect may be partly accounted for by widening the two sided metalization by half the thickness of the piezoelectric in each end, for the calculations.

The neutral axis in the platelet is used to establish the boundary conditions between platelets. Its position z_n, see Fig. 2, is defined as the position where the stress and strain in the composite is zero in pure bending with V = 0.

The deflection of the membrane is denoted by w(x), positive in +z direction.

To establish the boundary conditions at the ends of the platelets, we must relate the moment M in the platelet about its neutral axis and the elongation Δx of the platelet in x at the neutral axis, to the applied voltage V, the second derivative in x of w due to bending alone, ($\partial^2 w(x)/\partial x^2|_b$), and the dynamic stretching force F_x in the platelet, see Fig. 2. We find:

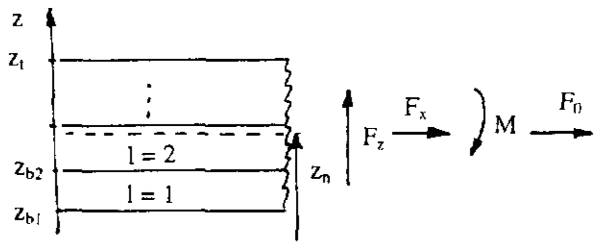

Figure 2: Cross section of a platelet with definitions.

$$M = VK_e - D_b \frac{\partial^2 w(x)}{\partial x^2}\Big|_b \qquad (1)$$

$$\Delta x = F_x / S^E - Ve_t / S^E$$

where

$$K_e = e_{eff} \sum_{l \in pv} (z_{b,l} + h_l/2 - z_n) \mathrm{Sign}(-P_{z,l}E_{z,l})$$

$$S^E = \sum_l C_{eff,l} h_l / (x_e - x_b) \qquad (2)$$

$$e_t = e_{eff} \sum_{l \in pv} \mathrm{Sign}(-P_{z,l}E_{z,l})$$

and $l \in pv$ means that the sum is taken over all piezoelectrics with applied voltage in the composite, and $\mathrm{Sign}(-P_{z,l}E_{z,l})$ is +1 when the electric field from a positive applied voltage and the polarization direction of the piezoelectric are in opposite directions, -1 otherwise. Further x_b and x_e are the start and end x positions of the platelet, and $C_{eff,l}$ is, for layer l, the proper elastic modulus for a strain in x direction which is uniform in z and at a constant voltage V, and h_l is the height of layer l.

The shear stiffness of the platelet in z-direction per unite length in y, is designated G_t, and gives the derivative of w(x) due to shear deformation as the shear force $F_x(x)$ divided by G_t. For the given piezoelectric symmetry this shear is not piezoelectrically coupled. The numerical value of G_t is found from an energy argument, according to [4], assuming that plane cross sections of the platelet remains plane under load, as:

$$\tau(z) = \frac{F_z}{D_b} \int_{z_b}^{z} C_{eff}(z)(z - z_n)dz$$
$$G_t = F_z^2 \left(\int_{z_b}^{z_t} \frac{(\tau(z))^2}{G(z)} dz \right)^{-1} \qquad (3)$$

Here G(z) is the shear modulus of the materials in the composite and z_b and z_t are the coordinates of the bottom and top surface of the platelet. For a uniform plate one finds G_t to be $Gh_{tot}/1.2$, while for a composite of vastly different materials, as PZT and silicon nitride, the correction factor to the sum of Gh may be as large as 1.7.

correction factor to the sum of Gh may be as large as 1.7.

The differential equation for w(x) is then found including the effects discussed above, a constant stretching force in the plate, F_0, shear deformation and bending of the plate, and a pressure p in an adjoining medium on the +z side of the plate. We further assume the time dependence exp(jωt), and get

$$D_b^P \frac{d^4 w}{dx^4} - F_0^P \frac{d^2 w}{dx^2} - \omega^2 m w = -p + \frac{D_b}{G_t} \frac{d^2 p}{dx^2} \quad (4)$$

where

$$D_b^P = D_b(1 + F_0/G_t)$$
$$F_0^P = F_0 - \omega^2 m D_b / G_t \quad (5)$$

Here m is the mass per unite area of the platelet. The homogeneous form of this equation, with p = 0, has four solutions giving the homogeneous solution w_h. In addition we need a particular integral w_p of the inhomogeneous equation, which is easily found for the case when $p = p_0 \exp(-jk_p x)$. The general solution is then the sum of $w_h(x)$ and $w_p(x)$, and has four integration constants which must be determined from boundary conditions.

The supporting structures on both sides of the total plate are described by the 3 by 3 compliance matrices s_{ij}^L and s_{ij}^R for the left, or low x, and right, or high x, side respectively. The matrices relate the deflection, w^X, tilt due to bending, $dw^X/dx|_b^X$, and movement in positive x direction at the neutral axis of the adjoining platelet at the joint, Δx^X, to F_z^X, M^X, and F_x^X in the platelet at the joint, where X is L or R, through

$$\begin{pmatrix} w^X \\ dw/dx|_b^X \\ \Delta x^X \end{pmatrix} = \left(s_{ij}^X\right) \begin{pmatrix} F_z^X \\ M^X \\ F_x^X \end{pmatrix} \quad (6)$$

If the support structures on the left and the right side are symmetric about a line in z direction, the elements with indices 11, 22, 23, and 32 will change sign as X is changed from left to right while other elements remain constant.

The mechanical boundary conditions in the structure are now easily discussed. For each platelet we have 4 wave amplitudes to determine, in addition to the longitudinal force F_x which in our description is constant along the plate. Hence we need five boundary conditions for a single platelet, and four additional conditions for each added platelet in the structure. The latter four are obtained from conditions between the platelets, where the following four quantities have to be continuous:

$$w$$
$$\frac{dw}{dx}\Big|_b = \frac{dw}{dx} - \frac{F_z}{G_t}$$
$$M + F_x z_n \quad (7)$$
$$F_z = -D_b^P \frac{d^3 w}{dx^3} - \frac{m\omega^2 D_b}{G_t}\frac{dw}{dx} + \frac{D_b}{G_t}\frac{dp}{dx}$$

F_z is the shear force shown in Fig. 2. The five former conditions are obtained as follows. At the ends of the total plate the two first conditions in (7) applies, and in addition we must require that the total length of the plate fits in between the loaded fixtures, which requires:

$$\Delta x^L - \Delta x^R + \sum_n \Delta x^{(n)} + \sum_m \frac{dw}{dx}\Big|_b^m \left(z_{n,L}^{(m)} - z_{n,R}^{(m)}\right) = 0 \quad (8)$$

Here Δx^L and Δx^R comes from (6), $\Delta x^{(n)}$ is the Δx in (1) and the sum in n is taken over all platelets. The sum in m is taken over all boundaries between platelets, and $z_{n,L}^{(m)}$ and $z_{n,R}^{(m)}$ are the positions of the neutral axis to the left and to the right of the neutral axis at the left and right of the boundary m respectively. All the boundary conditions may now be expressed by the total deflection w, the pressure in the fluid p, the longitudinal force F_x, and the applied voltage V.

The current through a piezoelectric film, layer no l, in a transducer platelet is found to be

$$I_l = -j\omega \int_{x_b}^{x_e} D_{z,l}(x)\,dx\,\mathrm{Sign}(-P_{z,l}E_{z,l}) =$$
$$j\omega C_{f,l} V + j\omega \mathrm{Sign}(-P_{z,l}E_{z,l})(K_e \left[\frac{dw}{dx}\Big|_b\right]_{x_b}^{x_e} - e_{eff}\Delta x) \quad (9)$$

where

$$C_{f,l} = \varepsilon_{eff}^S (x_e - x_b)/h_l \quad (10)$$

Here $C_{f,l}$ is the capacitance of the film with no bending or elongation in x of the platelet. The total current is found by summing the current through all piezoelectric films, assuming that they are coupled in parallel.

FEM analysis

A membrane with fixed supports, similar to the experimental device shown in Fig. 4, has been analyzed both with the analytical method and a FEM program. Care has been taken in the way the support of the membrane is treated in the FEM to allow contraction and expansion of the membrane in the thickness direction at the support, while avoiding tilting and deflection. With this in place the series and parallel resonance's of the structure matches to about 0.3% for the two methods of analysis.

We have further used FEM to calculate the compliance's of the supports in the experimental device described below. Although the support region there is made of brass

with a top layer of PZT, the support is analyzed as the homogeneous brass structure shown in Fig. 3. This should still give reasonable results as the PZT and brass have similar mechanical properties. Only a static analysis is made, as dynamic effects will be small in this structure.

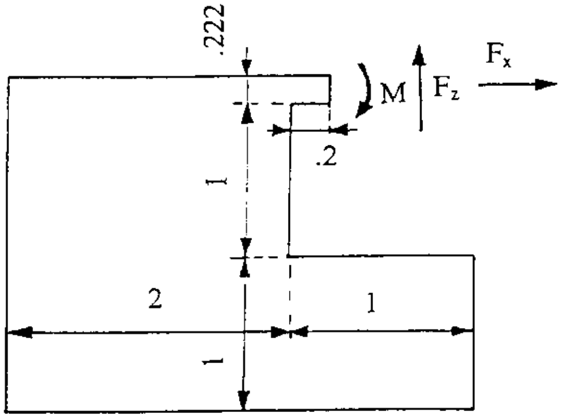

Figure 3. Cross section of support structure for FEM with forces and moment. Dimensions in mm.

The size of the support structure is a somewhat critical issue. For a static case it is easily shown that the support compliance's for translations with force and translation in the same direction, will diverge logaritmicaly as dimensions increase. In a real case this divergence is halted by reaction forces on other supports, and, at a high frequency, mass action. To treat this in an exact way is difficult as it includes radiation into the support, and is not attempted. Fortunately the compliance's involving tilting of the membrane at the support are the most important ones, and these may be shown to have a better convergence. The difference in resonance frequency using the compliance's from the shown support and one with height and width reduced by a factor of about 2 is less than 1%, compared to a 16% change from fixed to soft support. Hence a reasonable convergence is reached.

In the analysis the forces are applied on the shown membrane tip in Fig. 3, where also the deformations are observed. They are then transformed back to the root of the membrane using standard plate theory. The result is shown in Eq.(11), where the elements are given in SI units.

$$(s_{ij}^{L}) = \begin{pmatrix} 3.0\cdot10^{-11} & -7.0\cdot10^{-8} & -1.4\cdot10^{-11} \\ 7.7\cdot10^{-8} & -1.2\cdot10^{-3} & -5.4\cdot10^{-8} \\ -1.4\cdot10^{-11} & 5.4\cdot10^{-8} & 2.4\cdot10^{-11} \end{pmatrix} \quad (11)$$

Experiments

Two structures with the same cross section but with slightly different lengths, about 40mm and 49mm, where made and tested and the results compared with analysis. The cross section of the devices is shown in Fig.(4). For the brass we have used a density of 8640 kg/m^3, Young's modulus of 10.44*10^{10} Pa, and Poison's ratio 0.355. The PZT is of type 5h, and we have taken the material data from [5].

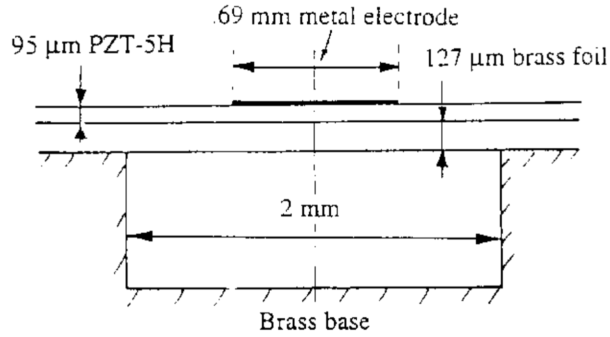

Figure 4: Cross section of test structure

For fixed supports and without acoustic loading the analytical model shows series and parallel resonance's for the structure of 183.6kHz and 188.7 kHz respectively. Using the support compliance's generated by FEM in the analytical model reduces the resonance's to 148 kHz and 153 kHz, still somewhat above the observed resonance's. By in addition increasing the total length of the membrane by .114 mm or about half the membrane thickness, the parallel resonance peak drops to 140 kHz, and hence matches the experiments. Adding loss terms, simulated as loading from a fluid without reactive effects, is used to bring the peak of the real part of the impedance down to the experimental values. The

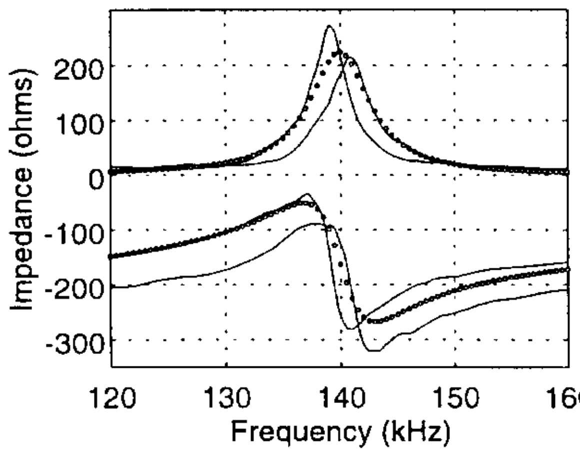

Figure 5: Measured, full lines, and calculated, o o, impedances of test device

resulting impedance's for the to experimental devices and the calculations are shown in Fig.(5). The impedance's are scaled to apply for a nominal device length of 40mm. We see that the theory gives a capacitance in between that of the two experimental devices, whereas it predicts a stronger piezoelectric coupling than observed in the experiments. Taking the product of the mechanical and electrical Q's of the devices as (an inverse) measure of coupling, we find this to be about 22 and 29 for the experimental devices compared to 16 in the calculations. The calculations clearly shows a higher coupling, even though there is a large difference in the two experimental results. The reasons fore these differences and the loss is not known. It could be due to inaccuracies in material parameters and manufacturing, but also to deficiencies in the modeling. The effects of radiation losses from the supports might be important, but also losses in the glue used to connect the PZT, brass foil and brass base.

Conclusion

An analytical model for a piezoelectrically driven flexural membrane transducer is presented. The model may handle arbitrarily layered plate structures without or with one or more piezoelectric layers. The model includes deformation due to shear forces, residual stress in the plate, and bending effects at height differences between plate elements or at the supports due to dynamic longitudinal forces in the membrane.

Resonance frequencies in a test structure with fixed supports are shown to match well with FEM calculations. FEM analysis is also used to calculate the compliance's of the supports in a PZT brass test structure. These are shown to be important for the resonance frequency of the structure, and brought the theoretical resonance's within 9% of the experimental results. Transducer capacitance is also modeled well, whereas the piezoelectric coupling is larger than in the experiments.

References

1. M.E. Vassergiser, A. N. Vinnichenko, and A. G. Dorosh: «Calculation and investigation of flexural-mode piezoelectric disk transducers on a passive substrate in reception and radiation», Soviet Physics Acoustics, 38 (6), pp 558-561, 1992.

2. G. Percin, L. Levin, and B. T. Khuri-Yakub: «Piezoelectrically actuated transducer and droplet ejector», IEEE Ultrasonics Symposium Proceedings, pp 913-916, 1996.

3. M. Lukacs, M. Sayer, D. Knapik, R. Candela, and F.S. Foster: «Novel PZT films for ultrasound biomicroscopy», IEEE Ultrasonics Symposium Proceedings, pp 901-904, 1996.

4. Flugge: «Handbook of Engineering Mecahnics».

5. B. A. Auld: «Acoustic fields and waves in solids», second ed. Krieger 1989.